[Frontiers in Bioscience, Landmark, 20, 716-727, January 1, 2015]

Differential effects of peripheral and transitional prostatic stromal cells on tumorigenesis

Bao Li[1], Yu-Bing Peng[1], Qi Chen[1], Juan Zhou[1], Ming Zhang[1], Hao Wang[1], Wen-JiLi[1], Jun Da[1], Zhong Wang[1], Yan Gao[2]

[1]Department of Urology, Ninth People's Hospital, School of Medicine, Shanghai Jiaotong University, Shanghai, [2]Department of Infectious Diseases, Huashan Hospital, Fudan University, Shanghai

TABLE OF CONTENTS

1. ABSTRACT

The human prostate contains two types of stromal cells, peripheral stromal cells (PSCs) and transitional stromal cells (TSCs). Here, we demonstrate the effects of PSCs and TSCs on tumorigenesis in prostate cancer (PCa) and identify the mechanisms underlying these effects. Using microarray analysis, we identified 3,643 differentially expressed genes in cocultures of TSCs, PSCs, and DU145 cells, a human prostate cancer cell line. Expression of cell division cycle 25 homolog A (CDC25A) was lower and that of tumor-associated calcium signal transducer 2 (TACSTD2) was higher in TSCs than in PSCs. Additionally, increased CDC25A expression or decreased TACSTD2 expression modulated the survival, growth, and migration of DU145 cells. These data suggest that PSCs promote and TSCs inhibit tumorigenesis by regulating the expression of CDC25A and TACSTD2.

2. INTRODUCTION

Prostate cancer (PCa) is the second leading cause of cancer-related death in the United States (1). Based on histological morphology, McNeal and Joshua *et al* proposed that the prostate is comprised of a peripheral zone (PZ), transitional zone (TZ), and central zone (2, 3). Benign prostatic hyperplasia occurs almost exclusively in the TZ, whereas in over 70% of cases, PCa occurs in the PZ. Less than 20% of PCas originate in the TZ, and PCas originating in the TZ exhibit a lower degree of malignancy than those originating in the PZ (4).

This paradoxical difference cannot be explained by morphology alone since the PZ and TZ are morphologically similar (2, 5). Different embryonic origins (6) and molecular characteristics likely play an important role. Indeed, differences in the gene expression patterns between the PZ and TZ have been described (7). However, anatomical differences make it difficult to build an *in vivo* experimental animal model replicating the clinical features of the PZ and TZ in prostate carcinogenesis.

The mesenchymal-epithelial interaction is induced by androgen-mediated embryological prostatic development (8). Stromal cells isolated from tumors, called carcinoma-associated stromal cells, can transform normal epithelial cells to neoplastic cells. Furthermore, normal stromal cells can be transformed into carcinoma-reactive stromal cells when cocultured with cancer cells (9). Some scholars have explained the differences in tumorigenesis between the PZ and TZ through this epithelial-stromal interaction (10).

In the current study, normal stromal cells from the PZ and TZ were cocultured with a hormone-independent PCa cell line, DU145, in an *in vivo* mouse model. The stromal cells from the PZ (termed peripheral stromal cells, or PSCs) enhanced the carcinogenicity of DU145 cells. In contrast, the stromal cells from the TZ (termed transitional stromal cells, or TSCs) inhibited DU145 carcinogenicity. This model provides a tool for examining the molecular mechanisms through which PSCs and TSCs affect prostate carcinogenesis.

3. MATERIALS AND METHODS

3.1. Isolation of stromal cells and culture

Fresh prostatic tissues were collected from healthy organ donors (age, 20–40 years) at the Shanghai Ninth People's Hospital (Shanghai, China). The experimental protocols were approved by the Shanghai Ninth People's Hospital Medical Ethics Committee. Stromal cells from the PZ and TZ were isolated and identified by two pathologists according to McNeal's zonal anatomy, as previously described (10, 11). Stromal cells were cultured at 37°C and 5% CO_2 in a humidified atmosphere in RPMI 1640 medium (Invitrogen, Carlsbad, CA, USA) supplemented with 10% fetal bovine serum (Gibco, Melbourne, Australia) and antibiotics including streptomycin (100 mg mL^{-1}) and 100 IU mL^{-1} penicillin (North China Pharmaceutical Co., Ltd, Shijiazhuang, China). Stromal cells at passages 3–5 were used. The androgen-independent PCa cell line, DU145 (American Type Culture Collection, Manassas, VA, USA), was cultured in RPMI 1640 medium containing 5% FBS.

3.2. *In vivo* analysis with a tumorigenesis model

Four- to five-week-old male athymic nude mice were obtained from the Animal Center of the Chinese Academy of Sciences (Shanghai, China). All mice were maintained in laminar airflow cabinets under pathogen-free conditions and cared for according to institutional guidelines. Twenty-seven nude mice were randomly divided into three groups and were subcutaneously injected as follows: group 1 (control, n = 9), inoculated with 2×10^6 DU145 cells in 0.2. mL phosphate-buffered saline (PBS) into the right flank; group 2 (n = 9), inoculated with 2×10^6 DU145 cells plus 2×10^6 PSCs in 0.2. mL PBS; and group 3 (n = 9), inoculated with 2×10^6 DU145 cells plus 2×10^6 TSCs in 0.2. mL PBS. Tumor dimensions were measured weekly, and tumor volumes were calculated as length × $width^2/2$. After eight weeks, the mice were killed, and the tumors were resected, cleaned, and weighed.

3.3. Immunohistochemical staining and terminal deoxynucleotidyl transferase (TdT) dUTP nick end labeling (TUNEL) assay

The resected tumors were fixed with 10% buffered formalin and 70% ethanol. Paraffin-embedded specimens were then sectioned at 5-mm thickness and stained with hematoxylin and eosin (HE) using standard histopathological techniques. Immunohistochemical staining for Ki67 antigen (Epitomics, CA, USA) was performed as previously described (12). Briefly, the sections were deparaffinized in xylene, and rehydrated using a graded alcohol series. Slides of normal tissue samples from a prostate biopsy were used as negative and positive controls. The sections were pretreated for antigen retrieval by microwave irradiation for 14 min in 0.0.1 mol/L citrate-buffered saline (pH 6.0.). Endogenous peroxidase activity was blocked by incubation with 0.3.% hydrogen peroxide for 10 min. Subsequently, the sections were incubated overnight at 4°C with mouse monoclonal antibodies against Ki67. The following day, detection was carried out using the streptavidin-biotin complex/horseradish peroxidase method with a HISTOFINE SAB-PO (M) or (R) Immunohistochemical Staining Kit (Nichirei, Tokyo,

Japan) according to the manufacturer's instructions. The sections were counterstained with Mayer's hematoxylin. Stained sections were analyzed using a light microscope (400× magnification; Olympus, Tokyo, Japan) connected to a video recorder that was linked to an Image-Pro Plus V6.0. computerized image system (Media Cybernetics, MD, USA). Apoptosis in tumor cells was analyzed using a TdT FragEL DNA fragmentation detection kit (Merck, Darmstadt, Germany) according to the manufacturer's instructions.

3.4. RNA extraction, complementary DNA (cDNA) microarray, and data analysis

Total RNA was extracted using either TRIzol reagent (Invitrogen) or an RNeasy kit (Qiagen, Valencia, CA, USA) according to the manufacturers' protocols. Following quality confirmation, RNA samples were amplified and labeled using a NimbleGen One Color DNA Labeling kit (Roche, Madison, WI, USA). RNA was then hybridized (NimbleGen Hybridization System, Roche, Madison, WI, USA) to a human genome array (12 × 135 K array; Roche) containing oligos representing 45,033 human genes. After washing, the processed slides were scanned with an ELx800 absorbance microplate reader (Biotek Instruments Inc., Winooski, VA, USA). NimbleScan (version 2.6., Roche NimbleGen, Madison, WI, USA) was used for data analysis, including quantile normalization and background correction. Agilent GeneSpring software (Agilent Technologies, Santa Clara, CA, USA) was used to further analyze the gene summary files. Three samples were randomly selected from each group for microarray analysis. The genes were considered differentially expressed when the ratio was >1.5. or <0.6.7 in normalized intensity between the two groups or when *P*-values were less than 0.0.5 by one-way analysis of variance (ANOVA).

3.5. Quantitative real-time reverse transcription polymerase chain reaction (RT-qPCR) analysis

Total RNA was extracted from cultured cells using TRIzol reagent or from tumor tissues using an RNA prep Pure Tissue Kit (TIANGEN Biotech, Beijing, China) according to the manufacturers' instructions. RNA was then quantified using the ratio of optical densities at 260/280 nm (OD_{260}/OD_{280}) obtained by an ultraviolet spectrometer. Total RNA (1 μg) from each sample was immediately reverse transcribed at 42°C for 60 min followed by inactivation at 94°C for 5 min. RT-qPCR was then performed with a Rotor-Gene6000 Real Time Thermal Cycler (Corbett Research Australia) and SYBR Premix Ex Taq (TaKaRa, Shiga, Japan) in accordance with the manufacturer's protocol. The following primers were used: human CDC25A (174 base pairs (bp)): forward, 5′-GGCAGTGATTATGAGCAACCA-3′, reverse, 5′-CAACAGCTTCTGAGGTAGGGA-3′; human TACSTD2 (219 bp): forward, 5′-CTGAGCCTACGCTGCGATG-3′, reverse, 5′-GGCCTTCTGAGACGTGTTCTG-3′; and β-actin (205 bp): forward, 5′-AGCGAGCATCCCCCAAAGTT-3′, reverse, 5′-GGGCACGAAGGCTCATCATT-3′. Reactions were performed in 25-μL volumes containing 12.5. μL SYBR Green, 5 × 10^{-6} μM forward and 5 × 10^{-6} μM reverse primers, and 2 μL cDNA. The cycling conditions were as follows: 2 min at 95°C and 40 cycles each of 95°C for 15 s, 55°C for 20 s, and 72°C for 45 s. The threshold cycle number was determined for all reactions, and in most cases, the threshold was manually adjusted to lie within the exponential phase using Rotor-Gene Real-Time Analysis Software 6.1. mRNA expression levels for each gene were calculated using the $2^{-\Delta\Delta CT}$ method, and the values were expressed as relative arbitrary units.

3.6. MTT assay

Cell growth and survival were evaluated by MTT assay according to established protocols. In short, cultured cells were incubated with MTT at the indicated time points. The absorbance of samples in the wells was read directly at of 570 nm.

3.7. Western blot

Cultured cells were lysed in RIPA lysis buffer. Cell lysates were subjected to sodium dodecyl sulfate polyacrylamide gel electrophoresis (SDS-PAGE) and immunoblotting with antibodies against cell division cycle homolog A (CDC25A) and tumor-associated calcium signal transducer 2 (TACSTD2).

3.8. Annexin V and propidium iodide (PI) staining

Cells were stained with Annexin V and PI (BD Biosciences) according to the manufacturer's instructions. Briefly, single-cell suspensions were resuspended in 1× Annexin V binding buffer at 1 × 10^6 cells/mL, and 1 × 10^5 cells were then stained with 5 μL Annexin V and PI for 15 min prior to flow cytometry analysis.

3.9. Cell cycle analysis

Cells were fixed in cold 70% ethanol for 30 min at 4°C. For analysis of the cell cycle

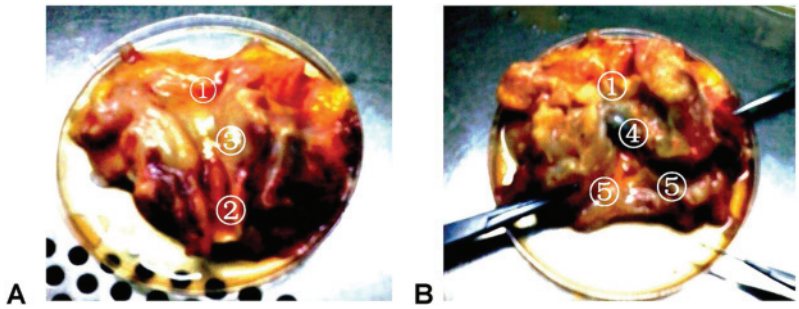

Figure 1. PSCs and TSCs isolated from the peripheral zone of the normal human prostate show fibroblast-like morphology after *in vitro* adherent culture. A) The prostate was positioned with the internal urethral orifice opened. B) An incision was made through the vertical axis of the urinary tract, and tissues near the posterior prostate capsule indicated the peripheral zone. 1, The cystic triangle area; 2, verumontanum; 3, urothelium covering the transitional zone; 4, seminal vesicle; 5, peripheral zone of the prostate.

distribution, cells were then treated with ribonuclease and stained with 200 µL PI.

3.10. Transfection and establishment of stable cell lines

DU145 cells were transfected with CDC25A- or TACSTD2-overexpression plasmids or short hairpin RNA (shRNA) constructs. The transfected cells were selected with G418 for 3 months.

3.11. Statistical analysis

All data were expressed as the mean and standard error of the mean (± SEM). Differences between groups were analyzed using the one-way ANOVA. All statistical analyses were performed using GraphPad Prism 5, and differences with *P*-values of less than 0.0.5 were considered statistically significant.

4. RESULTS

4.1. The effects of PSCs and TSCs on tumor growth

PSCs and TSCs showed fibroblast-like morphology following *in vitro* adherent culture. The prostate was positioned in a Petri dish with the internal urethral orifice cut exposed, and an incision was made through the vertical axis of the urinary tract (Figure 1). Tissues near the posterior prostate capsule were considered to represent the PZ. In the *in vivo* model of tumor growth after coculture of PSCs or TSCs with DU145 cells *in vivo*, we found that the volume and weight of tumors in group 2 were significantly higher than those in groups 1 and 3, when measured 28 days after cell injection ($P <$ 0.0.5). However, the volume and weight of tumors in group 1 were higher than those in group 3 after 9 weeks (Figure 2). These results indicated that PSCs exerted growth-stimulatory effects on DU145 cells *in vivo*, while TSCs exerted inhibitory effects.

4.2. Immunohistochemistry assessment

As shown in Figure 3, the tumors from groups 2 (Figure 3A2) and 3 (Figure 3A3) had more fibrous stromal tissue than those of group 1 did (Figure 3A1). Tumors from groups 1 and 3 showed a significantly lower level of Ki67 than those from group 2 ($P <$ 0.0.5; Figure 3B1–3). However, no differences in TUNEL signals were observed among the three groups ($P >$ 0.0.5; Figure 3C1–3), suggesting that enhanced cell proliferation was a key property conferred by co-injection of PSCs and DU145 cells, and not by injection of DU145 cells alone or co-injection of TSCs and DU145 cells.

4.3. cDNA expression analysis and RT-qPCR verification of differentially expressed genes

To elucidate the molecular alterations in tumor cells following stromal cell co-injection, and gene expression profiles were compared among tumors from the three groups using microarray analysis. A total of 3,643 genes showed statistically significant differences in expression ($P <$ 0.0.5). For example, 2,172 genes were upregulated and 1,471 genes were downregulated in cells from group 2 relative to those from group 1, while 2,337 genes were upregulated and 1,306 genes were downregulated in cells from group 1 relative to those from group 3. The genes encoding CDC25A and TACSTD2 were selected to verify the involvement of the DNA duplication- and cell cycle-associated pathways. RT-qPCR analysis showed that *CDC25A* gene expression was lower, while *TACSTD2* expression was higher in tumor cells from group 3 compared to those from group 2 (Figure 4A–C).

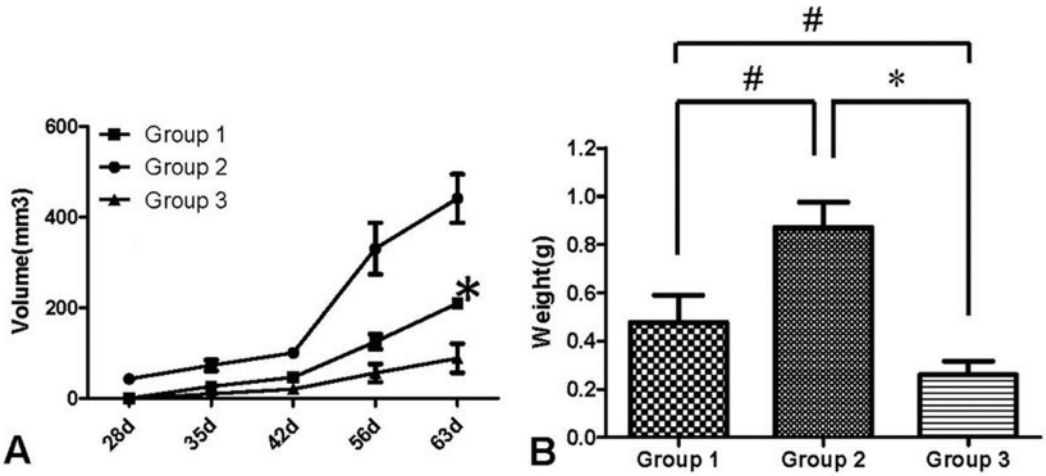

Figure 2. Co-injection of PSCs and TSCs with DU145 cells promotes tumor growth *in vivo*. A) DU145 cells were subcutaneously injected into athymic nude mice either alone (Group 1, N=9) or together with isolated PSCs (Group 2, N=9) and TSCs (Group 3, N=9). The tumor volume was monitored weekly until week 9 after injections. B) After isolation, representative tumors from Groups 1, 2 and 3 were photographed. Tumor weights from Groups 1, 2 and 3 were measured following isolation and expressed as mean ± SEM. **P* < 0.0.1, #*P* < 0.0.5.

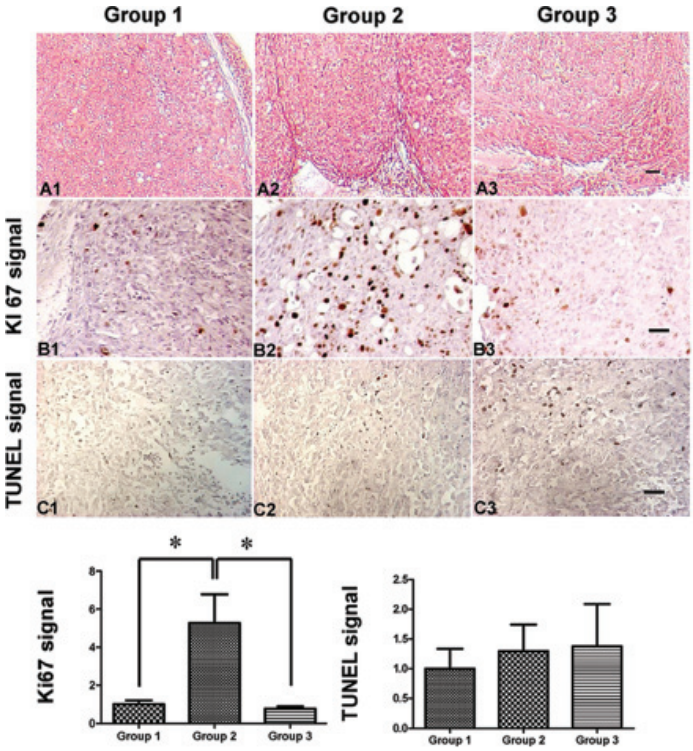

Figure 3. Co-injection of PSCs with DU145 cells promotes *in vivo* cell proliferation when TSCs are inhibited. A1, 2, 3) Tumor tissues were immunostained with hematoxylin and eosin. A marked increase in the dense fibrous tissue stroma was observed (B1, Group 2 and C1, Group 3) (scale bar, 200 mm) compared with DU145 cells alone (A1, Group 1); the Ki67 (B1, 2, 3) and TUNEL (C1, 2, 3) signals were quantified and compared among the three groups. The corresponding signal in Group 1 was arbitrarily defined as 1. **P* < 0.0.5, as compared to Group 1 (scale bar, 100 mm).

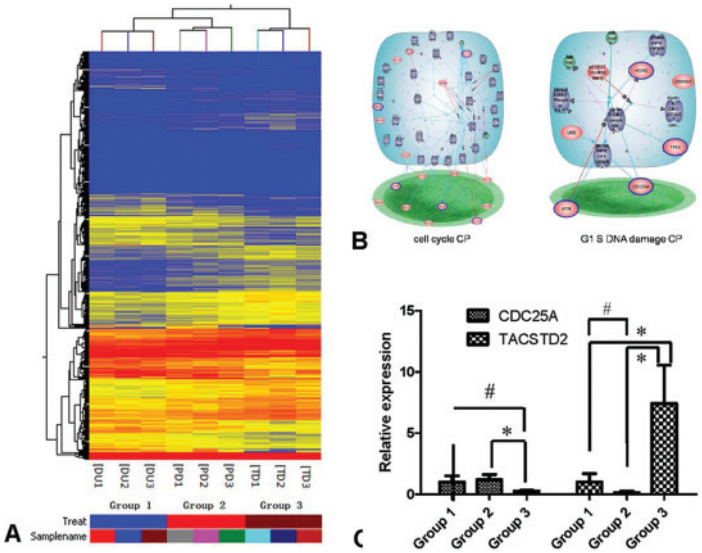

Figure 4. cDNA expression analysis and qRT-PCR analysis of target genes. A) Heatmap for hierarchical clustering of differentially expressed genes. B) Based on G0 and pathway analysis, the cell cycle and G1/S DNA damage CP was highly expressed. C) The expression of indicated target genes was examined by qRT-PCR analysis and presented as a ratio to internal control gene (β-actin), with the expression level in cells from Group 1 arbitrarily defined as 1. **P* < 0.0.1, #*P* < 0.0.5.

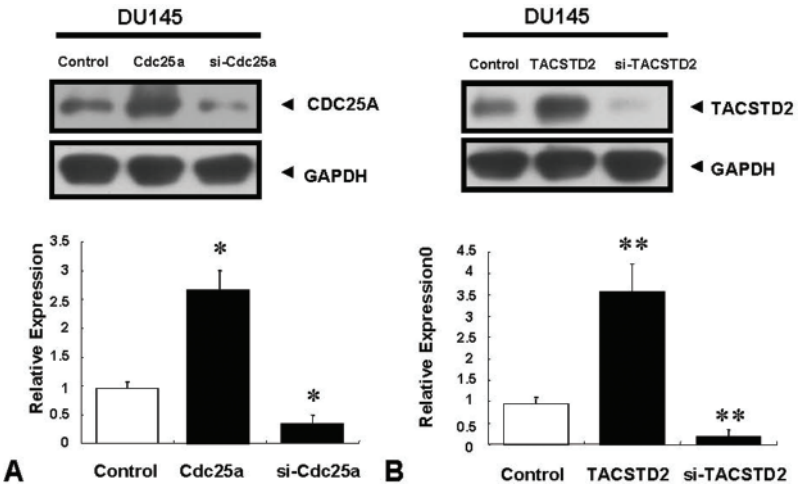

Figure 5. Stable overexpression or knock-down of CDC25A/TACSTD2 in DU145 cells. A) Western blot analysis of CDC25A or TACSTD2 expression in stable cell lines. B) The graph represents average intensities of gray of the protein in the indicated cell lines. All data are representative of three independent experiments. **P* < 0.0.5, ***P* < 0.0.1.

4.4. Increased CDC25A expression and reduced TACSTD2 expression promoted tumor growth and survival

To evaluate whether upregulation of CDC25A and downregulation of TACSTD2 could explain the observed changes in tumor growth and survival, we established stable cell lines by overexpressing or knocking out these two genes in DU145 cells. Western blot analysis confirmed that both overexpression and knockdown cell lines had significantly altered expression of CDC25A and TACSTD2 (Figure 5). CDC25A-overexpressing

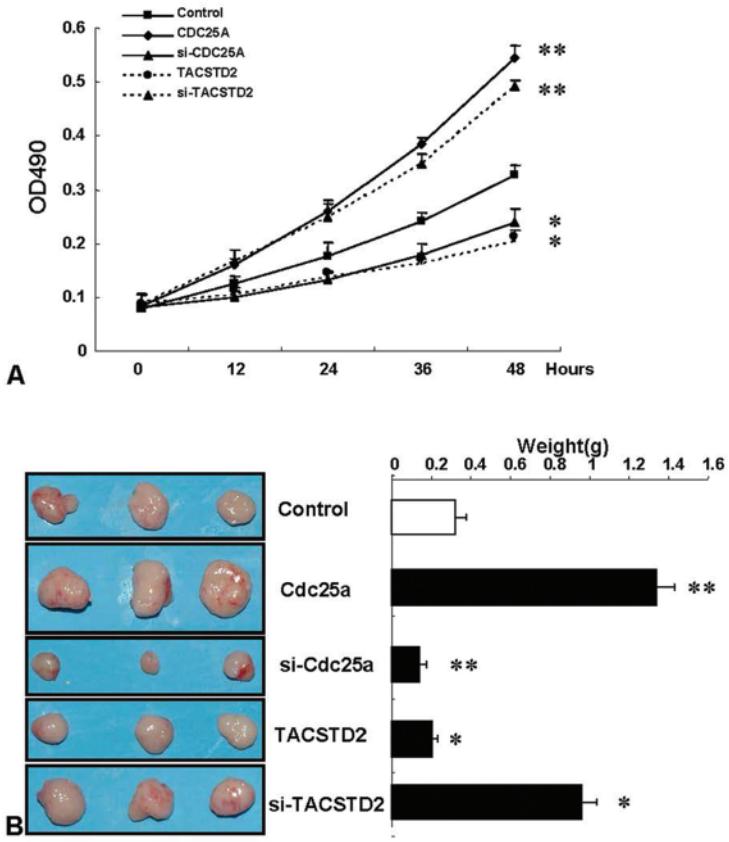

Figure 6. CDC25A and TACSTD2 regulate the survival and growth of DU145 cells. A) CDC25A or TASCTD2 up/down-regulated cells were incubated with MTT at the indicated time points and analyzed by ELISA. B) Modified cells were subcutaneously injected into athymic nude mice as indicated. The tumor volume was monitored weekly until week 9 post-injection. All data are representative of three independent experiments. *P < 0.0.5, **P < 0.0.1.

or TACSTD2-knockout DU145 cells showed significantly enhanced the survival, whereas cells in which CDC25A expression was downregulated or TACSTD2 was upregulated showed markedly reduced survival (Figure 6A). The growth rate was significantly higher in cells CDC25A-overexpressing or TACSTD2-knockout cells than in control cells; conversely, the growth rate was markedly reduced in cells exhibiting downregulation of CDC25A or upregulation of TACSTD2 (Figure 6B). These results indicated that changes in the expression of CDC25A or TACSTD2 were sufficient to modulate the survival and growth of DU145 cells.

4.5. CDC25A and TACSTD2 controlled apoptosis in DU145 cells

We further analyzed apoptosis using flow cytometry in DU145 cells exhibiting varying expression of CDC25A and TACSTD2. Upregulation of CDC25A or downregulation of TACSTD2 significantly reduced apoptosis in DU145 cells, while downregulation of CDC25A or upregulation of TACSTD2 consistently and significantly increased apoptosis in DU145 cells (Figure 7).

4.6. CDC25A and TACSTD2 controlled the cell cycle distribution in DU145 cells

The cell cycle of DU145 cells with altered of CDC25A or TACSTD2 expression was analyzed. The number of cells in the growth 2 (G_2)/mitosis (M) phase of the cell cycle was significantly increased in CDC25A-overexpressing or TACSTD2-knockout DU145 cells (Figure 8). Conversely, downregulation of CDC25A or upregulation of TACSTD2 resulted in a decreased

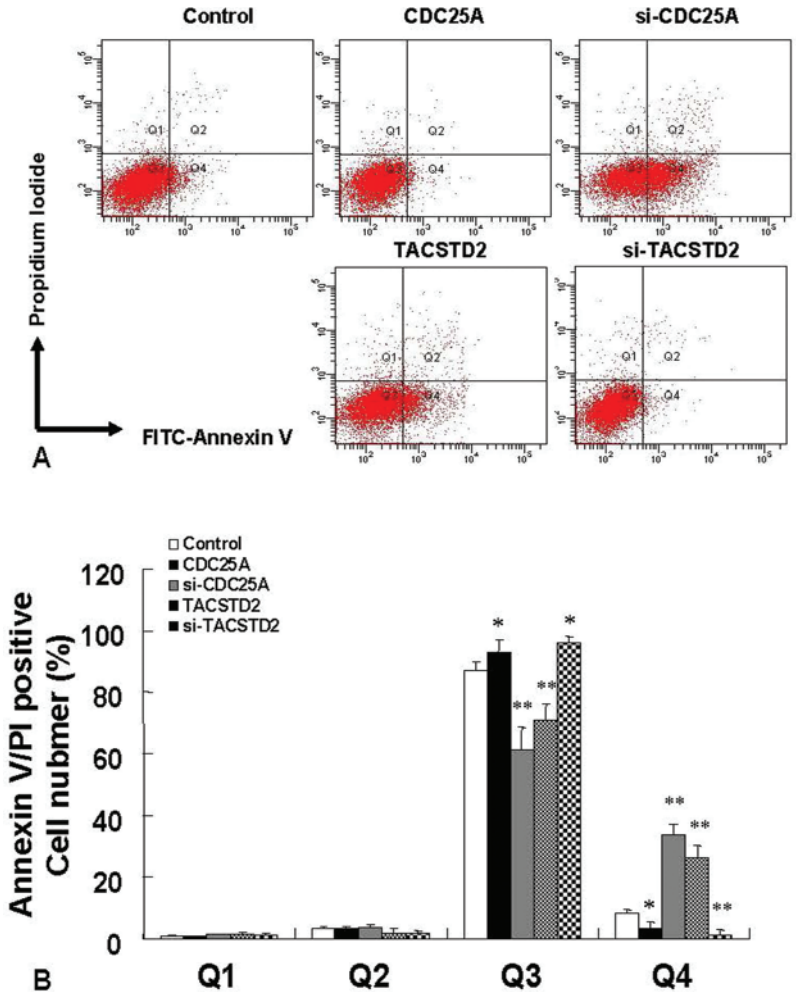

Figure 7. CDC25A and TACSTD2 regulate the apoptosis of DU145 cells. A) The apoptosis of CDC25A/TACSTD2 modified DU145 cells was evaluated by AnnexinV/PI staining. B) Statistical analysis of AnnexinV/PI staining of cells in A. All data are representative of three independent experiments. *P < 0.0.5, **P < 0.0.1.

number of cells in the synthesis (S) phase and an increased number of cells in the growth 1 (G_1) phase (Figure 8).

4.7. CDC25A and TACSTD2 regulated the migration of DU145 cells

We also conducted cell migration assays for CDC25A-overexpressing and TACSTD2-knockout DU145 cells. These cells showed significantly increased migration (Figure 9). Consistent with this, CDC25A-knockout or TACSTD2-overexpressing DU145 cells showed significantly reduced migration ability (Figure 9). Our results indicated that overexpression of CDC25A and downregulation of TACSTD2 promoted tumor growth and survival, whereas suppression of CDC25A expression and overexpression of TACSTD2 inhibited tumor growth. These findings may explain the observed effects of PSCs and TSCs.

5. DISCUSSION

In this study, we developed an *in vivo* model to show the opposing effects of isolated, normal stromal cells from the PZ and TZ on prostate carcinogenesis in DU145 cells. Stromal cells from the PZ have been shown to stimulate the growth of cancer cells *in vivo* (10), whereas cells from the TZ had the same albeit relatively weaker effect. In previous studies, similar results were obtained using PC3 prostate cancer cells cocultured *in vivo*

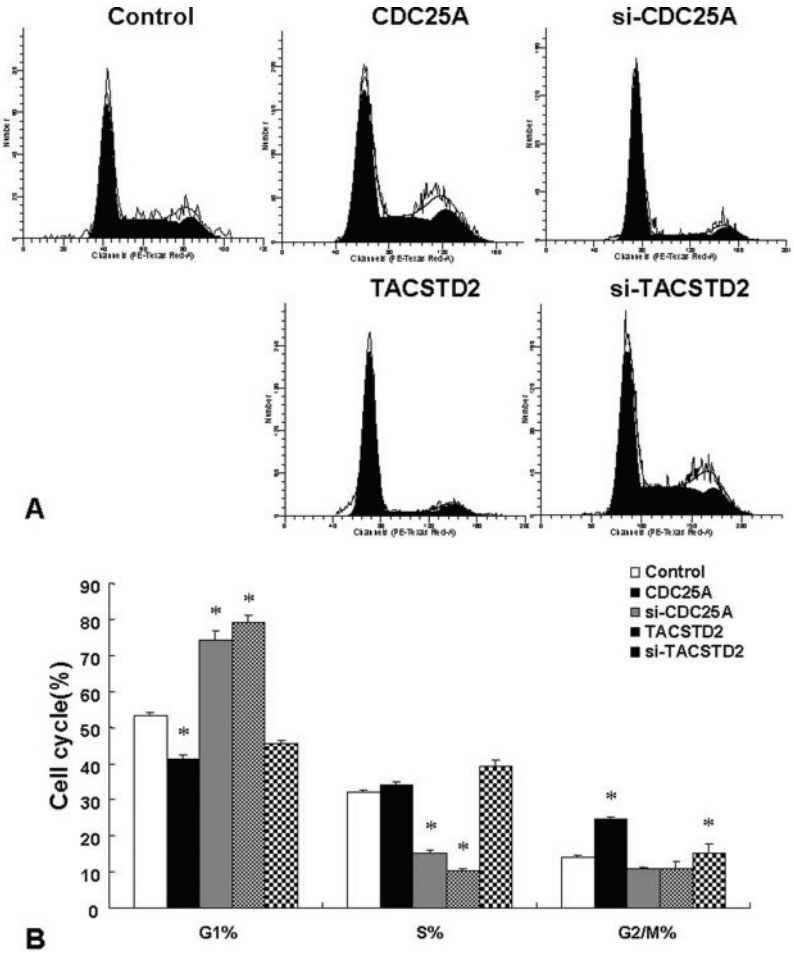

Figure 8. CDC25A and TACSTD2 regulate the apoptosis of DU145 cells. A) The cell cycle of CDC25A/TACSTD2 modified DU145 cells was evaluated by PI staining. B) Statistical analysis of PI staining of cells in A. All data are representative of three independent experiments. **P* < 0.0.5, ***P* < 0.0.1.

with stromal cells. Here, we used DU145 cells, which grow independent of androgen signaling. In contrast, PC3 cells exhibit low acid phosphatase and testosterone-5-alpha reductase activities. The androgen receptor (AR) is expressed both in stromal and epithelial cells in the prostate, and its expression can be enhanced in a coculture system (14). This overexpression may lead to inhibition of tumorigenesis by TSCs cocultured with AR-negative DU145 cells, as demonstrated in this study. In this study, the largest tumor in group 3 was smaller than the smallest tumors in groups 1 and 2, demonstrating the inhibitory effect of TSCs in this coculture system. Therefore, we hypothesize that the hormonal action of stromal cells might be beneficial for epithelial tumors.

Recent studies have demonstrated that normal prostate, PCa, and benign prostate hyperplasia tissues exhibit differential gene expression patterns (15, 16). In this study, gene expression analysis revealed the varying effects of PSCs and TSCs on epithelial carcinogenesis; our investigations focused on the metabolism and DNA duplication in these cells. Transforming growth factor (TGF)-β, c-myc, and p53 control CDC25A, which stimulates cell proliferation by promoting the transition from the G_1/S phase to the S and G_2/M phases of the cell cycle. Furthermore, CDC25A is highly expressed in PCas (17, 18). TACSTD2 is a potential stem cell marker of the prostate and it is expressed at higher levels in prostatic intraepithelial neoplasia than in PCas due to the hypermethylation

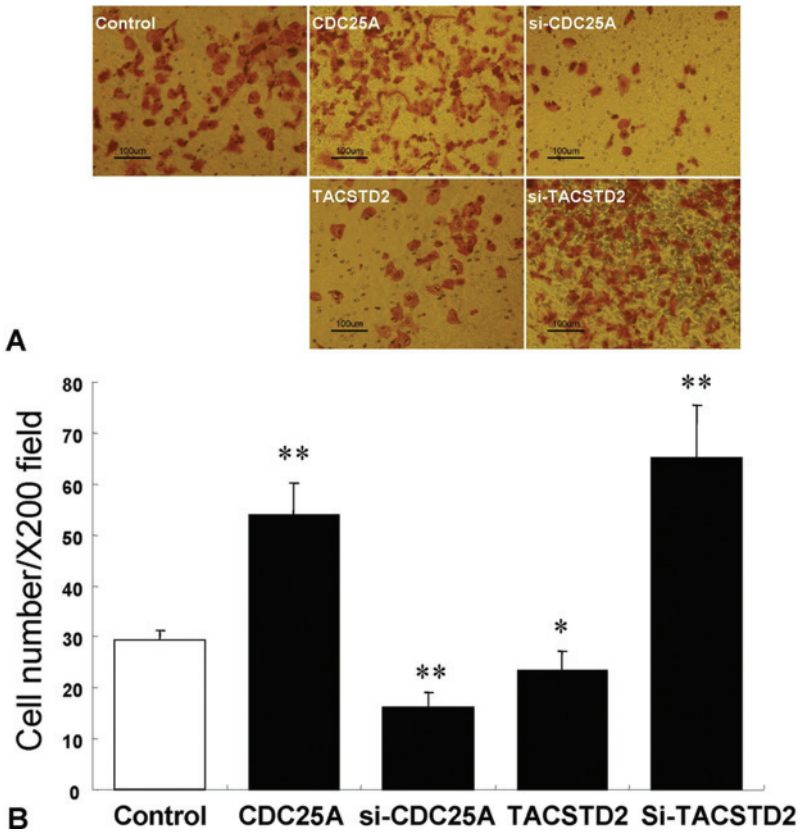

Figure 9. CDC25A and TACSTD2 regulate the migration of DU145 cells. The migration of CDC25A/TACSTD2 modified DU145 cells was evaluated by transwell assay. A) Microscopic analysis of transwell assay results (scale bar, 100 mm). B) Statistical analysis of the results of transwell assays. All data are representative of three independent experiments. *P < 0.0.5, **P < 0.0.1.

of TACSTD2 in PCas (19, 20). This implies that TACSTD2 may induce the transformation of epithelial tumor cells into normal cells. The higher expression of TACSTD2 in group 3 indicated that stromal cells isolated from the TZ of normal prostate tissues may affect carcinogenesis by inhibiting the growth of epithelial tumor cells. We found that PSCs upregulated CDC25A expression and suppressed TACSTD2 levels in tumors, promoting tumor cell survival, growth, and migration, whereas TSCs reversed the expression patterns of these two genes in tumors, thereby inhibiting their survival, growth, and migration. These behaviors indicated that stromal cells modulate the tumor microenvironment to control tumorigenesis by regulating the expression of oncogenes and tumor suppressor genes.

In a previous study, castrated nude mice, which were subjected to the same procedures as group 1 and group 2 animals in the present study, showed no carcinogenesis (11). Although DU145 cells can grow well in hormone-free medium *in vitro*, their proliferation is limited in the internal environment of the castrated animals. In the TSC-DU145 coculture model, tumor growth was inhibited; however, the stromal-epithelial effect may be the result of a more complex underlying relationship. The model proposed here may provide a useful tool to study the relationship between the hormone-stromal and stromal-epithelial effects.

Further studies are needed to determine whether the opposing effects of PSCs and TSCs cocultured with cancer cell lines in nude mice can be duplicated *in vitro*. If culture in an androgen-free medium affects the proliferation of the stromal-epithelial system, then elucidating the underlying mechanism may explain the anatomical variations observed during prostate carcinogenesis.

7. REFERENCES

1. JemalA, SiegelR, XuJ:CancerStatistics. 2010.CA Cancer J Clin 60, 277-300 (2010)
DOI: 10.3322/caac.20073
2. McNeal JE: The zonal anatomy of the prostate. Prostate 2, 35-49 (1981)
DOI: 10.1002/pros.2990020105
3. Joshua AM, Evans A, van der Kwast T: Prostatic preneoplasia and beyond. Biochim Biophys Acta 1785, 156-81 (2008)
Doi not found.
4. Pavelić J, Zeljko Z, Bosnar MH: Molecular genetic aspects of prostate transition zone lesions. Urology 62, 607-13 (2003)
DOI: 10.1016/S0090-4295(03)00501-6
5. Xia SJ, Tang XD: Apoptosis androgen receptor isoforms and androgen estrogen level in normal prostatic ductal system and prostatic hyperplasia. Chin J ExpSurg 20, 113-5 (2003)
Doi not found.
6. Laczko I, Hudson DL, Freeman A, Feneley MR and Masters JR: Comparison of the zones of the human prostate with the seminal vesicle: morphology, immunohistochemistry, and cell kinetics. Prostate 62, 260-6 (2005)
DOI: 10.1002/pros.20149
7. ShaikhibrahimZ, Lindstrot A, Ellinger J: Genes differentially expressed in the peripheral zone compared to the transitional zone of the normal human prostate and their potential regulation by ETS factors. Mol Med Report 5, 32-36 (2012)
Doi not found.
8. Cunha GR: Role of mesenchymal-epithelial interactions in normal and abnormal development of the mammary gland and prostate. Cancer 74, 1030-44 (1994)
DOI: 10.1002/1097-0142(19940801)74:3+<1030::AID-CNCR2820741510>3.0.CO;2-Q
9. Recavarren RA, Chivukula M, Carter G, Dabbs DJ: Columnar cell lesions and pseudoangiomatous hyperplasia like stroma: is there an epithelial-stromal interaction? Int J ClinExpPathol 3(1), 87-97 (2010)
Doi not found.
10. Zhao FJ, Han BM, Yu SQ, Xia SJ: Tumor formation of prostate cancer cells influenced by stromal cells from the transitional or peripheral zones of the normal prostate. Asian J Androl 11(2), 176-82 (2009)
DOI: 10.1038/aja.2008.33
11. Peng YB, Zhou J, Gao Y: Normal prostate-derived stromal cells stimulate prostate cancer development. Cancer Sci 102(9), 1630-5 (2011)
DOI: 10.1111/j.1349-7006.2011.02008.x
12. Nagao K, Yamamoto Y, Hara T, Komatsu H, Inoue R, Matsuda K, Matsumoto H, Hara T, Sakano S, Baba Y, Matsuyama H: Ki67 and BUBR1 may discriminate clinically insignificant prostate cancer in the PAS range <4ng/ml. Jpn J ClinOncol 41, 555-564 (2011).
DOI: 10.1093/jjco/hyq233
13. Scholzen, T. &Gerdes, J: The Ki-67 protein: from the known and the unknown. J Cell Physiol 182, 311-22 (2000)
DOI: 10.1002/(SICI)1097-4652(200003)182:3<311::AID-JCP1>3.0.CO;2-9
14. Niu YN, Xia SJ:Stroma–epithelium crosstalk in prostate cancer. Asian J Androl 11, 28-35 (2009)
DOI: 10.1038/aja.2008.39
15. Kim YJ, Yoon HY, Kim SK: EFEMP1 as a novel DNA methylation marker for prostate cancer: array-based DNA methylation and expression profiling. Clin Cancer Res 17(13), 4523-30 (2011)
DOI: 10.1158/1078-0432.CCR-10-2817
16. Hanson JA, Gillespie JW, Grover A, *et al*. Gene promoter methylation in prostate tumor-associated stromal cells. J Natl Cancer Inst 98(4), 255-61 (2006)
DOI: 10.1093/jnci/djj051

17. Galaktionov K, Chen X, Beach D: CDC25 cell-cycle phosphatase as a target of c-myc. Nature 382(6591), 511-517 (1996) DOI: 10.1038/382511a0

18. Chiu YT, Han HY, Leung SC, Yuen HF, Chau CW, Guo Z, Qiu Y, Chan KW, Wang X, Wong YC, Ling MT: CDC25A functions as a novel Arcorepressor in prostate cancer cells. J Mol Biol 385(2), 446-56 (2009) DOI: 10.1016/j.jmb.2008.10.070

19. Goldstein AS, Lawson DA, Cheng D, Sun W, Garraway IP, Witte ON: Trop2 identifies a subpopulation of murine and human prostate basal cells with stem cell characteristics. Proc Natl Acad Sci U S A 105(52), 20882-7 (2008) DOI: 10.1073/pnas.0811411106

20. Jeronimo C, Esteller M: DNA methylation markers for prostate cancer with a stem cell twist. Cancer Prev Res 3(9), 1053-5 (2010) DOI: 10.1158/1940-6207.CAPR-10-0131

Abbreviations: PSCs, stromal cells from the peripheral zone; TSCs, stromal cells from the transitional zone; PCa, prostate cancer; BPH, benign prostatic hyperplasia; PZ, peripheral zone

Key Words: Prostate, Normal, Cancer, Peripheral Zone, PSCs, TSCs

Send correspondence to: Zhong Wang, Department of Urology, Ninth People's Hospital, School of Medicine, Shanghai Jiaotong University, Shanghai, China, Tel: 86-13585920101, Fax: 86-21-23271667, E-mail: zhongwang2010@tom.com